

# Magnetic Sensor Used to Detect Contamination of Insulating Oil in Motors Applied to Electrical Submersible Pump

Filipe Quintaes, Andrés O. Salazar, André L. Maitelli, Francisco Fontes, Madson A. A. Vieira, and Thiago Esley

Departamento de Computação e Automação, Universidade Federal do Rio Grande do Norte, Natal RN 59072-970, Brazil

This paper presents a solution for detecting contamination of insulating oil used in the artificial lift method of the oil-type electrical submersible pump (ESP), which indirectly protects the induction motor associated with that system. The objective of this sensor is to generate an alarm signal at just the moment when the contamination in the isolated oil is present. The prototype was designed to work in harsh conditions to reach a depth of 2000 m and temperatures up to 200°C. It used simulator software to define the mechanical and electromagnetic variables. Results of field experiments were performed to validate the prototype. The final results performed in an ESP system with a 60-HP motor showed a good reliability and fast response of the prototype.

**Index Terms**—Induction motor, isolate oil, magnetic sensor, oil contamination.

## I. INTRODUCTION

THIS paper presents a solution for detecting contamination of insulating oil used in the artificial lift method of the oil-type electrical submersible pump (ESP). This method is one of the most important for the petroleum industry at present, and it operates with large flows and high depths. However, this method has a problem, which is the frequent burning of the induction motor due to contamination of insulating oil [1]. These burns cause unplanned interventions in the process of petroleum extraction, generating economical and time losses.

In this method, the subsurface equipment is subdivided into the pump, electric motor, electric cable, and seal protector. The seal has several functions such as mechanically connecting the pump shaft and the motor shaft, withstanding the axial force of the pump, equalizing the internal motor pressure with the pressure of the fluids produced by them, and providing the necessary volume for motor oil expansion caused by the heat generated while it is in operation. Its main function, however, is to protect the induction motor, preventing the motor oil from by-production oil being contaminated, and consequently be burned. The seal with the continuous work causes the onset of motor oil contamination, which leads to the loss of its insulating property. In accordance [2], the statistics show that the induction motor has the highest failure rate by oil contamination. This contamination causes problems to the induction motor due to short-circuiting.

Through the industrial interest, new ideas emerged as solutions these problems. One of these is for a magnetic coupling model that transmits twisting force to the pump motor, thereby eliminating the use of a rubber seal [3]. Another is a seal for applications under unfavorable environmental conditions, such as the presence of sand and solids, corrosive fluids, and high temperatures (up to 218°C) [4].

This paper presents a new solution for this problem, having technical and economic feasibility and advantages for itself compared to other alternatives.

Manuscript received February 21, 2011; accepted May 01, 2011. Date of current version September 23, 2011. Corresponding author: F. Quintaes (e-mail: filipe@dca.ufrn.br).

Color versions of one or more of the figures in this paper are available online at <http://ieeexplore.ieee.org>.

Digital Object Identifier 10.1109/TMAG.2011.2154359

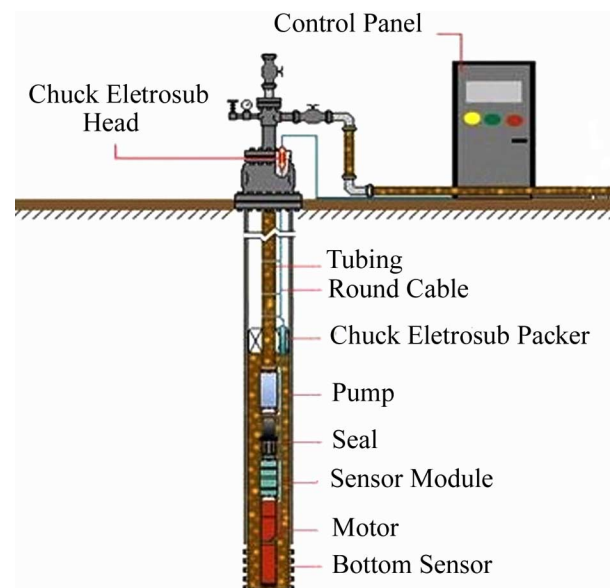


Fig. 1. Location of the sensor module in an ESP system.

The main objective of this paper will enable the petrochemical industry to adopt a predictive maintenance system, reducing operating costs and maintenance due to the reduction in the number of corrective interventions since each corrective intervention is about \$110 million [5].

## II. SENSOR DESIGN

The sensor module is inserted between the motor and the protective seal and consists basically of a detector of electric oil contamination by the variation of electric conductivity between a pair of electrodes, as shown in Fig. 1. The work environment is extremely hostile, operating at a depth of 2500 m with a temperature of 200°C. Due to the difficulties encountered in the delivery of power from the surface, the system was designed without the need for an auxiliary power system.

Fig. 2 shows the electric schematic of the sensor magnetic. The monitoring, detection, and transmission system are done by an electromechanical assembly. This system has two permanent magnets, one coil, an insulating transformer (T1), one

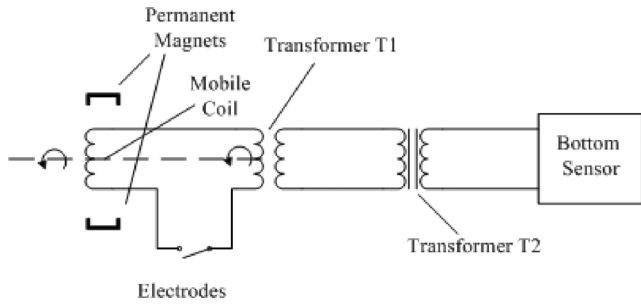


Fig. 2. Electric schematics of the sensor magnetic.

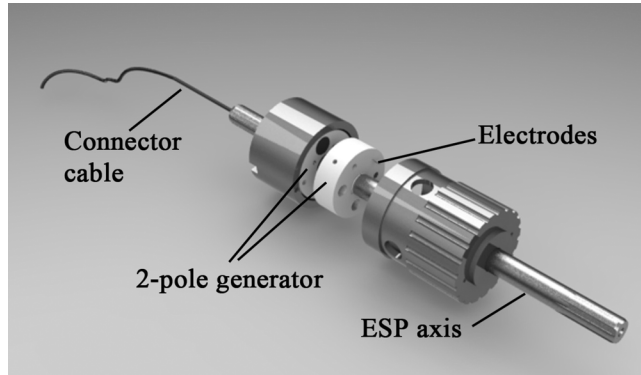


Fig. 3. Housing mechanical of the sensor module.

transformer (T2) responsible for signal conditioning, and one electronic module identified as the bottom sensor.

The magnets together with the coil work as a synchronous generator. The magnets are installed on a fixed housing ESP module, and the coil is installed on the shaft of the motor rotating speed of the motor. The transformer T1 serves to transmit the signal of contamination at the moment that the impedance of the electrodes decreases. The primary coil of this transformer T1 will be spinning at synchronous speed, while the secondary coil is fixed in the system ESP. The transformer T2 is responsible for signal conditioning and protection of the electronic module of the bottom sensor.

The mobile coil is connected to the T1 transform with a cable going through the hollow of the shaft. When the mobile coil is rotating over a magnetic field generated by the permanent magnets, it produces an electromotive force between its terminals. When the contamination is present, the circuit is closed in the electrodes terminals, and the sign goes to the bottom sensor circuit through the T1 and T2 transformers.

The principle of detecting contaminants in the insulating oil consists of amplitude variation in the voltage signal generated as a function of the variation in the physical-chemical characteristic of the medium in which the electrodes are found. A thorough dimensional survey of all the components of the ESP system was made. It was observed that it would be necessary to introduce a small module to fit the magnetic sensor into the current structure of the ESP system. This module was designed with enough space to house the magnetic sensor and other necessary mechanical structures. Fig. 3 shows the new module designed.

The designed transformers used in the sensor development aimed to work with the power levels required were specified

TABLE I  
TRANSFORMER PARAMETERS

Device	R1(Ω)	R2(Ω)	X1(Ω)	X2(Ω)	R <sub>0</sub> (Ω)	X <sub>m</sub> (Ω)
T1	0,29	0,03	0,46m	0,05m	13,8	78,3
T2	19,2	11,3	1,10	0,65	185	1017

T1 = transformer T1, T2 = transformer T2, R1 = primary resistance, R2 = secondary resistance, X1 = leakage reactance of primary winding, X2 = leakage reactance of secondary winding, X<sub>m</sub> = exciting reactance e R<sub>m</sub> = exciting resistance.

plates oriented crystals, to T1 core transformer, for presenting core losses of 1.3 T with 2 W/Kg. The T2 core transformer was specified martensitic steel A440, which is the same material as the axes of the ESP system. The project was developed in accordance with [6], Table I presents the results of the equivalent circuit model T.

The level of induced voltage in the transformer T1 will serve as a premise for the generator project. The specification of the magnet used was based taking into account the temperature of the operation system and maximum performance of the magnet within the project boundaries. It has a magnetic flux full density of 1.15 T with operating temperatures of 200°C [6].

The specification of the generator coil was based on the function of the relative permeability of the material. It used the model of cylindrical ferrite since it has a relative permeability of about 2000 [6]. The physical design of the inductor is based on the Faraday–Neumann’s law. Specific technical relations are important for the inductor volt-amps and the relation between magnetic induction and magnetic field [2], then the number of windings (*N*) of inductor is

$$N = \frac{L \cdot I_{peak}}{B_{max} \cdot Ae} \quad (1)$$

where:

- N* number of windings;
- B<sub>max</sub>* magnetic flux density maximum;
- L* inductance;
- I<sub>peak</sub>* current maximum;
- Ae* cross-sectional area of the core of the coil.

The maximum current density, *J<sub>max</sub>*, is given by:

$$J_{max} = \frac{N \cdot I_{rms}}{Ap} \quad (2)$$

where:

- Ap* cross-sectional area of the copper winding;
- I<sub>rms</sub>* effective current of the inductor.

Since the wires have circular geometry, windings occupy only a certain area of the available window. Thus, it is necessary to define a constant *K<sub>w</sub>* designed “load factor of copper inside the reel.” The typical value of the constant *K<sub>w</sub>* for the construction of inductors is 0.95, according to [7], but this can change depending on the geometry of the conductors used.

Thus, *K<sub>w</sub>* can be defined as

$$K_w = \frac{Ap}{Aw} \quad (3)$$

Setting the constant  $K_w$ , we can rewrite (2) as follows:

$$N = \frac{J_{\max} \cdot K_w \cdot A_w}{I_{\text{rms}}}. \quad (4)$$

Equating (1) and (4)

$$\frac{J_{\max} \cdot K_w \cdot A_w}{I_{\text{rms}}} = \frac{L \cdot I_{\text{peak}}}{B_{\max} \cdot Ae}. \quad (5)$$

Thus, it defines the value of the product areas ( $A_w \cdot Ae$ ) required for the construction of the inductor

$$A_w \cdot Ae = \frac{L \cdot I_{\text{peak}} \cdot I_{\text{rms}}}{J_{\max} \cdot K_w \cdot B_{\max}} \cdot 10^4. \quad (6)$$

The factor  $10^4$  in (6) was added to adjust the unit  $\text{cm}^4$ . For usual ferrite cores,  $B_{\max}$  value are around 0.3 T. The value of current density depends on the drivers used in the windings, and that typically used is  $450 \text{ A/cm}^2$ .

The core area was defined for a core diameter of 6.4 mm, with density and the driver set for a current of 0.158 A as defined in the design of the transformer, and it is possible to determine the number of turns through (4). As the operating frequency can be considered low, it has no problem related to skin effect. It can be determine through the section

$$S = \frac{I_{\text{rms}}}{J_{\max}}. \quad (7)$$

With the dimensional data of the core, calculation is performed by

$$V = \frac{\pi \cdot D^3 \cdot (h/D)}{4} \quad (8)$$

where

- $V$  volume of core ( $\text{m}^3$ );
- $D$  diameter of core (m);
- $h$  magnetic core height (m).

After determining the magnetic field generated in the center of a solenoid  $H$ , the determination of the density maximum field  $B_{\max}$  and the core area  $Ae$  is possible to determine the flux  $\Phi$  through

$$\Phi = B_{\max} \cdot Ae. \quad (9)$$

The induced voltage  $E_{\text{rms}}$  is determined by the frequency  $f$ , the number of turns  $N$ , and the magnetic flux  $\Phi$

$$E_{\text{rms}} = 444 \cdot \Phi \cdot f \cdot N. \quad (10)$$

The calculated values are listed in Table II.

To assess sensor reliability, US MIL-HDBK-217 F of 1991—Reliability Prediction for Electronic Induction motor Systems—was used. This norm proposes a reliability prediction method for electronic components without the need of conducting experimental analyses, based on the assessment of component reliability and on the flow of information between them during the operation of the system.

Thus, a mean time to flaw (MTTF) of approximately 76 000 h (8, 6 years) is gained.

TABLE II  
SUMMARY OF MAIN CHARACTERISTICS OF THE GENERATOR COIL

	Parameter	Variable	Value
Core	Length	L	20 mm
	Diameter	D	6,4 mm
Wire	Apparent permeability	$\mu_{\text{ap}}$	30
	Insulating wire diameter	$d_{\text{wire}}$	0,203 mm
	Wire diameter	$d_{\text{iso}}$	0,267 mm
Solenoid	Length	$l_{\text{wire}}$	132,5 m
	Magnetic flux	$\Phi$	$11 \times 10^6 \text{ Wb}$
	Average diameter	$d_{\text{sol}}$	11,2 mm
	Length	$l_{\text{sol}}$	20 mm
	Layers	$n_{\text{cam}}$	50
	Turns	$n_{\text{esp}}$	3787
Coil	Magnetic field strength	H	29917 A/m
	Magnetic flux density	B	1,15 T
	Voltage rms	U	11,7 V
	Resistance	R	70 $\Omega$
	Current	I	0,158 A
	Power dissipated	$p_{\text{dis}}$	1,8 W

Therefore, it must be qualified that although mean time to flaw is an indicator of the operational time of an electronic component or system, one cannot expect that most components produced will operate flawlessly for a period of time equal to MTTF. Although the MTTF of the sensor found is an estimated value, it gained a satisfactory result because current interventions in ESP systems are executed on average amount of time, normally after two years.

### III. SIMULATION RESULTS

The simulations were performed to validate and verify the design limits. This software is responsible for simulating (resolving) the electromagnetic origin using the finite element analysis (FEA) technique.

The induced voltage in the coil is determined from the rotation speed of magnetic flux and the number of turns of the inductor, according to (10). Knowing that the system speed remains unchanged and the number of turns is limited due to space limitations in the design, it performed simulations to obtain the desired magnetic flux varying the core of the inductor, the types of magnets, and the distance between the inductor and magnets. Table III shows the simulations were performed to generate induced voltage graphs summary by setting the system speed at 1800 rpm.

The samarium cobalt magnet (SmCo) was specified according to the results presented in Table III and the operational conditions of temperature. To meet the design requirements of samarium cobalt magnet (SmCo) became the most appropriate. These magnets have high coercive force, higher resistance to demagnetization, high standard of thermal stability (up to  $350^\circ\text{C}$ ), and resistance to corrosion and oxidation. Fig. 4 shows the distribution of magnetic field lines of the two magnetic poles with permanent magnets made of samarium cobalt, where it can be seen that the level of magnetic field intensity in the coil is around 0.03 T, which ensures a level field enough to induce an appropriate voltage.

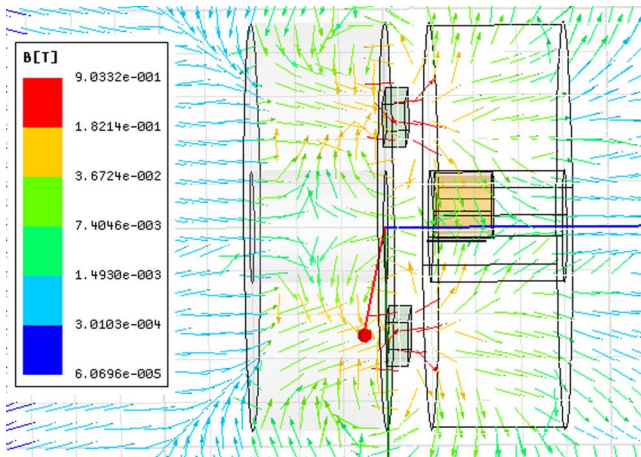


Fig. 4. Distribution of magnetic field lines of the 2-pole generator with magnets made of samarium cobalt.

TABLE III  
SUMMARY OF SIMULATION

Core Coil	Distance(mm)	Magnet	Number of Magnet	Induced Voltage rms (V)
Air	3	NdFeB	2	0.17
Ferrite	1	NdFeB	2	1.05
Ferrite	3	NdFeB	2	0.75
Ferrite	3	NdFeb	1	0.45
Ferrite	5	NdFeB	2	0.55
Ferrite	1	SmCo	2	0.96
Ferrite	3	SmCo	2	0.63
Ferrite	3	AlNiCo	2	0.37
Ferrite	5	AlNiCo	2	0.06

Distance = distance between the inductor and magnets.

#### IV. EXPERIMENTAL RESULTS

After analysis of the mathematical model, the mechanical design, and the simulations, the sensor module assembly was set up in the laboratory and in the field to validate the simulation results. In the practical laboratory procedure, the best coil position was analyzed to take advantage of the maximum number of field lines possible, providing a higher level of induced voltage.

Initially, a structure that could reproduce the simulations performed was set up. An assay using two magnets was then conducted. With the use of two magnets in the sensor module assembly, a greater influence from the magnetic field is observed, producing a more uniform waveform in the coil. Fig. 5 shows the voltage waveform obtained with two magnets.

The designed sensor was tested for performance evaluation. Tests were performed with the provisions of the ESP system horizontally without coupling the sensor to acquire the background variables of both voltage and current transformers.

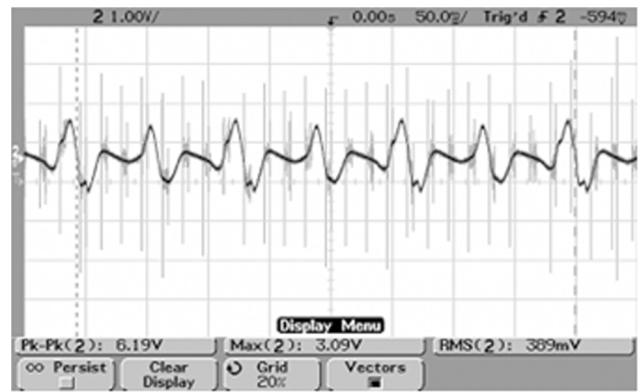


Fig. 5. Output of the sensor module in the state of contamination.

The test with the ESP system requirements of a vertical was planned and executed, and their results showed a 32-s time to record contamination. In this test, we used an induction motor 4 pole with a power of 60 HP and working with a speed of 1800 rpm.

#### V. CONCLUSION

The prototype sensor designed and implemented has been tested in operational conditions (temperature, pressure, and contaminants) from a typical ESP demonstrating its technical feasibility of use. The sensor proved to be robust, having a quick answer and great reliability.

The results obtained in this paper should be of great interest to the petrochemical industry, given that operational and maintenance costs will be reduced.

#### REFERENCES

- [1] N. W. Hein, Jr., J. D. Clegg, and S. M. Bucaram, "Recommendations and comparisons for selecting artificial lift methods," *J. Petroleum Technol.*, pp. 1128–1131, 1163–1167, Dec. 1992.
- [2] F. O. Quintaes, "Sistema de sensoriamento eletromagnético utilizado para detecção da contaminação do óleo isolante no motor do método de elevação artificial do tipo bombeio centrifugo submerso," Tese de Doutorado, UFRN, Natal-RN, Brazil, 2010.
- [3] G. L. Araux and S. E. Buchanan, "Sealed ESP motor system," US Patent 6863124, Aug. 03, 2005.
- [4] A. I. Watson and J. A. Booker, "Electric submersible pumping sensor device and method," US Patent 20090277628, Dec. 11, 2009.
- [5] A. C. Almeida, G. G. Monteiro, and I. A. Figueira, "Estudo de viabilidade técnica e econômica do campo Barba Negra," Dep. de Engenharia de Petróleo, Pontifícia, Universidade Católica, Rio de Janeiro, Brazil, V. 01, Jul. 2007.
- [6] W. Flanagan, *Handbook of Transformer Design and Applications*, 2nd ed. Boston, MA: McGraw-Hill, 1993.
- [7] I. Barbi, *Projetos de fontes chaveadas*, 2nd ed. Florianópolis, Brazil: INEP, 2001.